Effect of Filler Alloys on Heat-Affected Zone Cracking in Preweld Heat-Treated IN-738 LC Gas-Tungsten-Arc Welds

K. BANERJEE, N.L. RICHARDS, and M.C. CHATURVEDI

The effect of filler alloys C-263, RENÉ-41, IN-718, and FM-92 on heat-affected zone (HAZ) cracking susceptibility of cast IN-738 LC, which is a high-temperature Ni-based superalloy used at temperatures up to 980 °C and is precipitation hardened by the γ' (Ni_3Al,Ti) phase, by gas-tungsten-arc (GTA) welding was studied. In addition, autogenous welds were also made on the IN-738 parent material. The preweld treatments consisted of the standard solution treatment at 1120 °C for 2 hours followed by air cooling, and a new heat treatment, which was developed to improve the HAZ cracking resistance of IN-738 LC. This heat treatment consisted of solution treating at 1120 °C followed by air cooling then aging at 1025 °C for 16 hours followed by water quenching. Welds were observed to suffer intergranular HAZ cracking, regardless of the filler alloy; however, the autogenous welds were most susceptible to HAZ cracking. In general, the cracking tendency for both heat treatments was maximum for C-263 and RENE-41 fillers and decreased with the use of FM-92 and IN-718 filler alloys. The HAZ cracking was associated mainly with constitutional liquation of γ' and MC carbides. On some cracks, liquated low melting point containing Zr-carbosulfide and Cr-Mo borides were also observed to be present. The cooling portion of the weld thermal cycle induced precipitation hardening *via* γ' phase in the γ matrix of the weld metal. The HAZ cracking increased as the weld metal lattice mismatch between γ' precipitates and γ matrix of the weld and its hardness (Ti + Al) increased. However, the weld-metal solidus and solidification temperature range, determined by high-temperature differential scanning calorimetry, did not correlate with the HAZ cracking susceptibility. It is suggested that the use of filler alloys with small γ'-γ lattice mismatch and slow age-hardening response would reduce the HAZ cracking in IN-738 LC superalloy welds.

I. INTRODUCTION

IN-738* LC is a casting superalloy, which is precipitation hardened by $L1_2$-type γ' phase precipitates. It is extensively used in land-based power generation and aero-engine gas turbines due to its excellent high-temperature mechanical and corrosion/oxidation properties. However, in spite of its excellent properties, components made of IN-738 LC suffer damage on extended use in the extremely hostile environment that exists in high-temperature turbines. The high cost of new replacement parts has necessitated a need to repair these damaged components. The repair procedures often require the cracks to be welded, and the worn out parts to be built up by an overlay process. One of the major drawbacks of superalloys is their susceptibility to weld cracking. The weldability of superalloys containing large amounts of (Ti + Al), which are the required constituents of the main precipitation strengthening phase Ni_3Al-based γ', is particularly poor. Therefore, IN-738 LC superalloy with its Ti + Al concentration of 6 to 7 wt pct is an especially difficult to weld alloy.

*IN-738 LC is a trademark of INCO Alloys International, Huntington Woods, WV.

The extensive use of superalloys and a need to repair them has therefore resulted in a great deal of research being done to eliminate or minimize cracking in superalloy welds. However, in spite of the extensive use of IN-738 LC, where severe weld cracking occurs in the HAZ, a very limited amount of information is available on the mechanism of HAZ cracking.

Through studies done on several other superalloys, it is known that HAZ cracking, which is intergranular in nature, is affected by the (1) presence of precipitates on grain boundaries (carbide, boride, gamma prime, and other low melting phases), which may liquate and initiate cracking;[1,2,3] and (2) morphology of grain boundaries (planar or serrated),[4,5] which would affect the ability of an intergranular crack to propagate.

By careful analysis of the relationship between preweld microstructures and weld cracking susceptibility of IN-738 LC, Thakur *et al.*[6] developed a preweld heat-treatment process. This treatment results in reduced strength and improved ductility of the base alloy, combined with a discrete distribution of $M_{23}C_6$ precipitates on the grain boundaries, which inhibits propagation of an intergranular crack. This heat treatment has been observed to significantly reduce the HAZ cracking as compared to the solution-treated IN-738 LC alloy, which is the traditional preweld heat treatment. Another commonly used method of preventing HAZ cracking in this alloy is to use dissimilar, but low strength and ductile filler alloys, such as INCONEL* 625, which is nonage hardenable. Therefore, the resulting welds, though crack free, or with a minimum number of cracks, have relatively inferior

*INCONEL, RENE-41, and FM-92 are trademarks of INCO Alloys International, Huntington, WV.

K. BANERJEE, formerly Postdoctoral Fellow, Department of Mechanical and Manufacturing Engineering, University of Manitoba, Winnipeg, MB, Canada R3T 5V6, is Research Scientist, Tata Iron and Steel Co., Jamshedpur, 831001 India. N.L. RICHARDS, Associate Professor, and M.C. CHATURVEDI, Distinguished Professor and Canada Research Chair, are with the Department of Mechanical and Manufacturing Engineering, University of Manitoba. Contact e-mail: mchat@cc.umanitoba.ca

Manuscript submitted March 26, 2004.

mechanical properties. Some authors[7–10] have also reported an improvement in HAZ cracking resistance of IN-738 LC by conducting special manual GTA welding, high-temperature electron beam welding, electron beam welding preceded by a preheat treatment, and plasma-transferred arc welding. However, the effect of the use of filler alloys with varying amounts of Ti and Al has not been reported previously. Therefore, a research project was initiated to study the effect of various types of filler alloys with varying concentration of Ti and Al on the HAZ cracking susceptibility of IN-738 LC superalloy. This study presents the effect of filler alloy C-263, RENE-41,* FM-92,* and IN-718 on HAZ cracking susceptibility of preweld heat-treated cast IN-738 LC superalloy.

II. EXPERIMENTAL

Coupons 15-cm long, 2.54-cm wide, and 0.6-cm thick of as-cast IN-738 LC were provided by Hitchiner Manufacturing Inc. of Milford, New Hampshire. The chemical composition of the as-cast material and that of the filler alloys is shown in Table I. Coupons 7.5 × 2.5 × 0.27 cm were cut from the as-received plates and V grooved by a numerically controlled wire electric discharge machine (EDM). The 45° groove was 0.125-cm deep. They were then given two preweld heat treatments: (1) solution treatment at 1120 °C for 2 hours followed by air cooling (ST) and (2) the preweld heat treatment developed by Thakur *et al*.[6] which consists of solution treatment at 1120 °C followed by air cooling, then aging at 1025 °C for 16 hours, followed by water quenching (UMT). The solution treatment at 1120 °C is below the gamma prime solvus of around 1180 °C for IN-738. The preweld heat-treated specimens were GTA welded in a single pass by Standard Aero Ltd. (Winnipeg, Canada) using 60 amps d.c. at 10 V, with welding and filler wire feed speed of 1.27×10^{-3} and 4.7 to 7.2×10^{-3} m/s, respectively. Autogenous welds on V-grooved specimens were also made using the same welding parameters. Nine sections of each weld, transverse to the welding direction, were metallographically prepared by polishing and the cracking susceptibility of welds was determined by measuring the average total crack length (average TCL) per section.

The mechanically polished samples were electrolitically etched in a mixture of 12 mL H_3PO_4, 40 mL HNO_3, and 48 mL H_2SO_4, and their microstructures were characterized by optical as well as scanning electron microscopy (SEM). The SEM analysis was carried out by a JEOL*-5900 LV scanning electron microscope equipped with an Oxford energy-dispersive X-ray spectrometer with ultra-thin window detector. Semiquantitative chemical analysis was done by using Oxford-INCA EDS analysis software. Crack lengths were measured by using Clemex image analysis software. Thin foils for transmission electron microscopy (TEM) examination were prepared by mechanical grinding, dimpling, and electropolishing 3-mm disc specimens by a Fishione twin jet electropolisher using 25 pct perchloric acid-75 pct methyl alcohol bath held at a temperature of −20 °C to −50 °C using a current of approximately 1.8 to 3.5 A. Thin foils were examined by a JEOL JEM 2000 FX transmission electron

*JEOL is a trademark of Japan Electron Optics Ltd., Tokyo.

Table I. Chemical Composition of the As-Cast and the Filler Alloys (Weight Percent)

Alloys	Al	Si	Ti	Cr	Mn	Fe	Co	Cu	W	Mo	Ta	Zr	B	C	S	P	Bi	Nb	Ni
As cast	3.52	0.04	3.42	15.75	<0.01	—	8.5	—	2.51	1.88	1.61	0.04	0.014	0.11	0.001	—	<0.0001	0.84	rem
Filler-RENE-41	1.5	0 to 0.5	3.1	19	0 to 0.10	0 to 5	11	—	—	10	—	—	0.005	0.09	0 to 0.015	—	—	—	55
Filler C-263	0.53	0.16	2.07	20.33	0.22	0.37	19.78	<0.01	—	5.88	6.1	—	0 to 0.005	0.07	<0.002	<0.005	—	—	51.22
Filler FM-92	0	<0.01	2.59	14.20	2.08	9.27	0.06	0.04	—	—	—	—	—	0.05	0.015	—	—	—	69.94
Filler IN-718	0.50	0.05	0.94	17.3	0.03	rem	0.03	0.01	—	2.97	—	—	0.004	0.05	0.001	0.003	—	5.08	52.9

microscope. Hardness of the base alloy, HAZ, and weld metal were measured by a Vickers hardness tester. A minimum of 10 hardness measurements was taken per sample.

High-temperature differential scanning calorimetry (DSC) of the weld metal was done on selected samples. For this, the weld-metal samples were carefully separated from the homogeneous portion of the fusion zone by wire EDM. The transformation energetics of the samples was measured using a NETZSCH DSC 404 C Pegasus (Burlington, MA) differential scanning calorimeter using alumina crucibles. The samples were surrounded by alumina powder to prevent contamination of the sample crucible. Alumina powder was also used as a reference material in the reference crucible. The temperature calibration was done by measuring the melting temperatures of high-purity aluminum, silver, gold, nickel, and cobalt reference samples. Prior to heating, the DSC system was evacuated and back filled with argon three times. The measurements were subsequently carried out in a flowing argon atmosphere. The mass of the samples was in the range of 84 to 98 mg. They were heated to 1500 °C at a rate of 20 °C/min, held for 5 minutes, and cooled to 600 °C at a cooling rate of 20 °C/min.

X-ray diffraction studies were performed to determine the lattice mismatch between the matrix γ and γ' precipitates in the weld metal by using a Rigaku diffractometer (Danvers, MA) operating in a continuous scanning mode using Cu $K_{\alpha 1}$ radiation ($\lambda = 0.154056$ nm) in the 2θ range of 10 to 140 deg.

III. RESULTS AND DISCUSSION

A. *Characterization of Preweld Heat-Treated Materials*

The microstructure of the ST air-cooled material consisted of primary cuboidal γ' particles in an fcc γ matrix (Figure 1). Coarse and fine secondary γ' precipitates formed on air cooling while finer γ' particles were only resolvable by TEM. Coarser γ' particles present between the primary γ' particles are seen in Figure 1. In the ST material, the size of primary γ' precipitates is between 0.25 and 0.7 μm and that of the secondary γ' particles is ~0.12 μm. A γ-γ' eutectic island covers about one-third of Figure 1, showing coarse γ' within the island. The UMT heat treatment on aging resulted in the coarsening of secondary γ' particles to 0.3 to 1 μm (Figure 2). The γ-γ' eutectic was present in both heat-treated conditions. In addition, discretely distributed particles, which were identified as $M_{23}C_6$ by EDS analysis, were also present at the grain boundaries (Figure 2). The Zr-rich carbosulfide and Cr-Mo–rich boride phase were also observed near γ-γ' eutectic islands. Examples of the Zr-rich carbosulfide phase in an ST specimen along with its EDS spectrum are shown in Figures 3(a) and (b), respectively, while Cr-Mo rich boride and its EDS spectrum are shown in Figures 4(a) and (b), respectively. In Figure 3(a), partially resolvable secondary γ' in the γ matrix can be seen between the eutectic and the Zr precipitate. The difference in the microstructure of the two differently preweld heat-treated materials was also reflected in their hardness, which for the ST material was 384 ± 4 and for the UMT material was 340 ± 5 VPN.

B. *Analysis of GTA Welds*

1. *HAZ cracking*

All the welds suffered cracking in the HAZ and no cracks were observed in the weld metal of any of the welds. The mode of cracking was mainly intergranular and an example of HAZ cracking is shown in Figure 5, which is an optical micrograph of a part of a weld section. The cracks were adjacent to the fusion boundary but were always located in the partially melted zone of the HAZ.

The average total crack length (Av. TCL) values for the autogenous and the filler weld, along with 2σ (standard deviation) values, in the ST and UMT preweld conditions are shown in Figure 6, along with average weld-metal hardness. It can be seen that the cracking resistance of welds with the filler alloys was better than that of the autogenous welds. The cracking susceptibility of FM-92 and IN-718 weldments was almost the same but significantly smaller than that observed in specimens welded with C-263 and RENE-41 filler alloys. The Av. TCL in C-263 and RENE-41 filler welds of the ST material was measured to be 0.9 to 1 mm, which reduced to

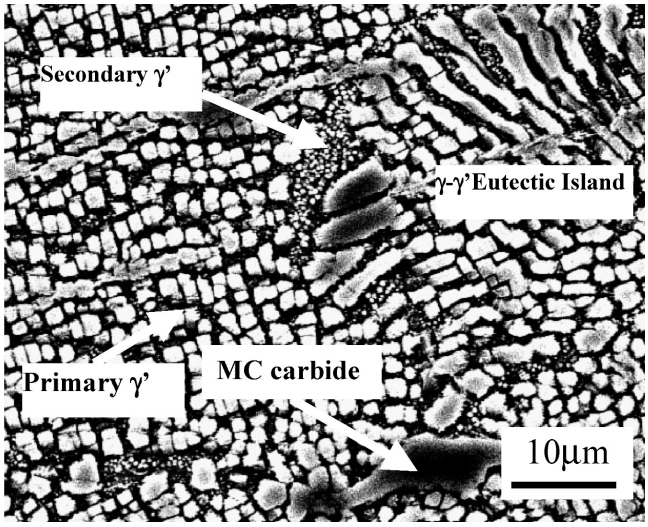

Fig. 1—SEM micrograph of ST material showing primary γ', secondary γ', and γ-γ' eutectic.

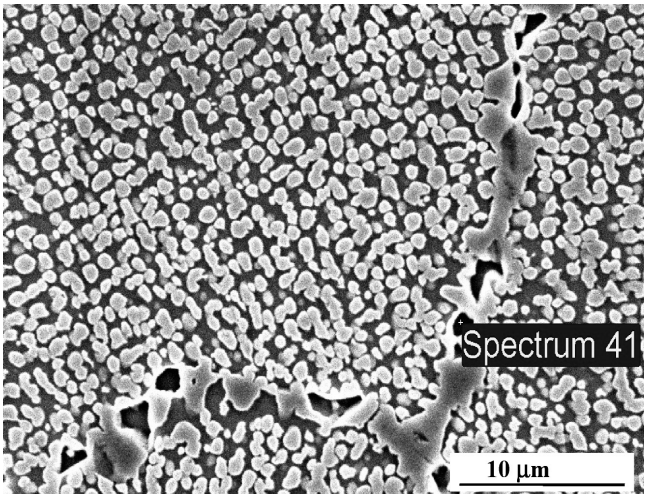

Fig. 2—SEM micrograph of UMT material showing secondary γ' particles along with $M_{23}C_6$ particles at grain boundaries.

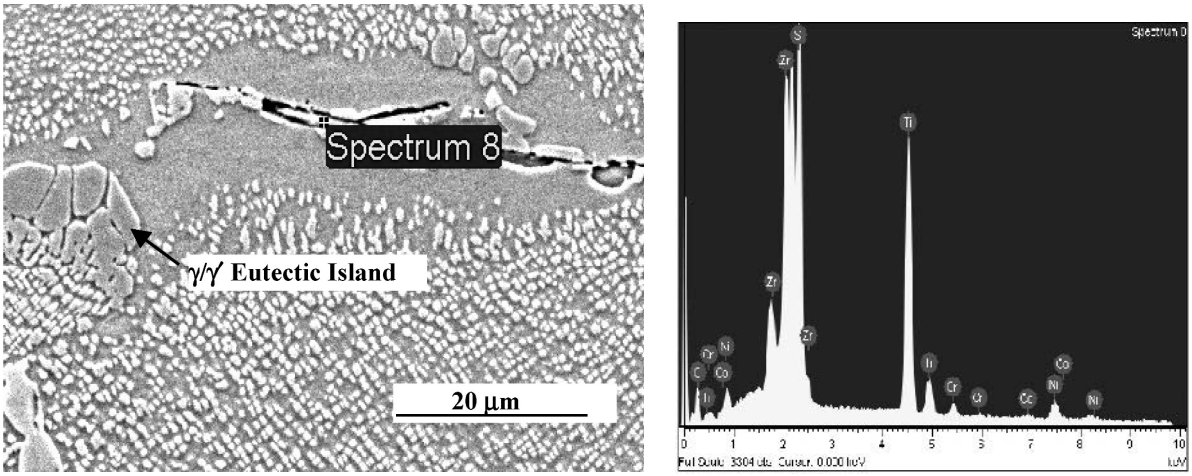

(*a*) (*b*)

Fig. 3—SEM micrograph of ST material showing (*a*) Zr-rich carbosulfide near γ-γ' eutectic and (*b*) EDS spectrum of Zr-rich carbosulfide.

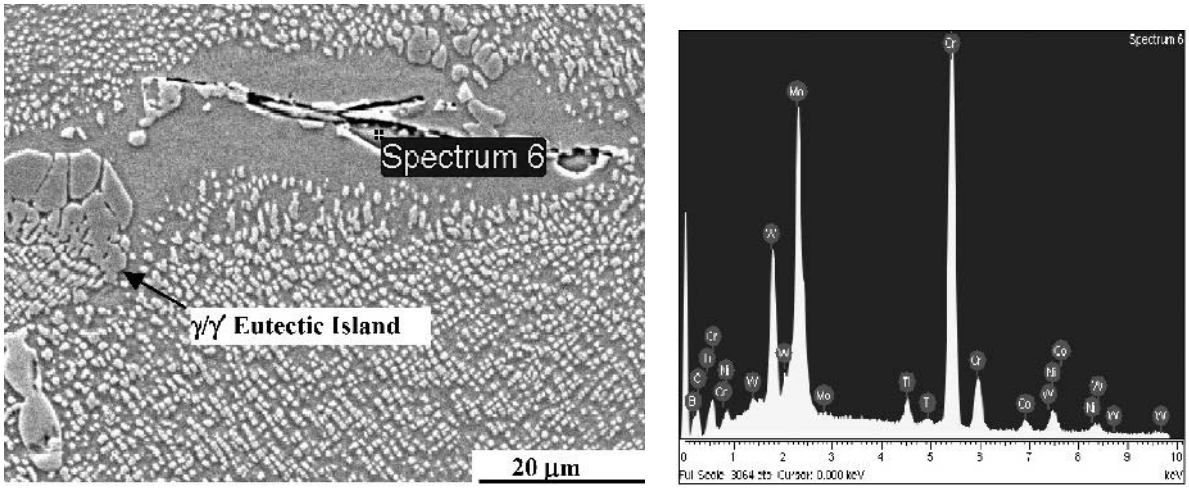

(*a*) (*b*)

Fig. 4—SEM micrograph of ST material showing (*a*) Cr-Mo boride near γ-γ' eutectic and (*b*) EDS spectrum of Cr-Mo boride.

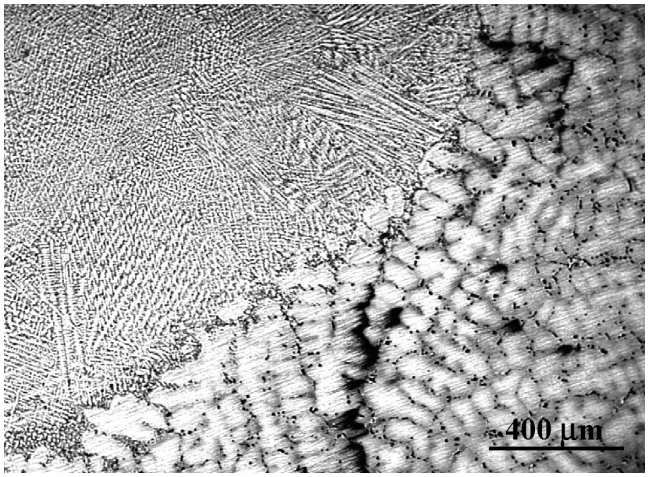

Fig. 5—Optical micrograph showing HAZ microfissuring.

around 0.3 mm with the use of FM-92 and IN-718 filler alloys. Similarly, in the UMT condition, the Av. TCL was measured to be about 0.1 mm in both the FM-92 and IN-718 filler alloy welds as compared to 0.4 to 0.5 mm in C-263 and RENE-41 filler welds. Thus, the cracking reduced significantly by using filler alloys as compared to the autogenous welds for both the heat-treated conditions, and the cracking susceptibility decreased by using different filler materials in the following order: C-263 $\approx$ RENE-41 $>$ FM-92 $\approx$ IN-718. It should also be noted that the susceptibility to cracking of the UMT preweld-treated material was consistently less than that of the ST material, regardless of the type of filler alloys used, as well as in the autogenous welds.

Figure 6 also shows an unusual phenomenon in that the UMT hardness values are consistently higher than the ST weld values. This has also been observed by us in a parallel investigation being currently done, but at present, the reason remains unclear.

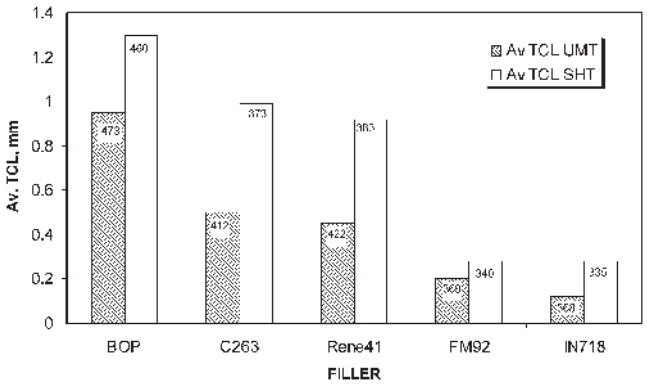

Fig. 6—Average TCL in weld made with different filler alloys. The hardness of the weld metal is also given in the histograms and 2σ values of Av. TCL.

2. *Microstructural analysis of welds*

To determine the reasons for dependency of HAZ cracking susceptibility of IN-738 LC on the nature of filler alloys, the microstructures of HAZ and weld metal were analyzed by optical and electron microscopy. The microstructural examination of HAZ revealed the presence of liquated γ', γ-γ' eutectic, MC carbides, Zr carbosulfide, and Cr-Mo–rich boride phases. These phases were present in both the preweld heat-treated materials. The nature and characteristics of liquated phases were not influenced by the type of filler alloy used, and they were also present in the autogenous welds. The liquated phases were distributed inter as well as intragranularly, and HAZ cracking was always associated with them. Liquated Zr-carbosulfide and Cr-Mo borides within the grains of the IN-718 filler weld HAZ were observed as seen in other superalloys.[11–15] The presence of constitutionally liquated γ' precipitates along a cracked boundary in the HAZ of ST material welded with RENE-41 filler is shown in the SEM micrograph in Figure 7(a), which was also previously reported by the present authors.[4] Liquation of the γ-γ' eutectic was also observed along the cracked grain boundaries in the HAZ of the UMT material welded with RENE-41 filler. A low melting point phase on a HAZ crack in a C-263 filler alloy weld, shown in Figure 7(b), was revealed by the X-ray maps (Figure 7(c)) to be a boride phase. A Cr-Mo–rich boride, adjacent to a cracked boundary, was also observed in the HAZ of a ST and RENE-41 welded material.

The microstructures of weld metal in welds made with different filler alloys were also examined. Examination by SEM revealed the presence of MC carbides in C-263, RENE-41, and FM-92 and also in IN-718 weld metals (Figures 8(a) through (c)). Occasionally, MC carbide particles were also observed to be associated with Laves/γ eutectic (Figure 8(c)). The semiquantitative chemical analyses determined by EDS of MC showed that the concentration of MC forming elements, Ti, Nb, and Ta, depended upon the type of filler used. The presence of Laves/γ eutectic in the weld metal of IN-718 filler weld is shown in Figure 8(d) By EDS analysis, this phase was found to be rich in Ni, Cr, Nb, and Mo (Table II). The semiquantitative chemical analyses of MC carbides by EDS showed that the concentration of MC forming elements, Ti, Nb, and Ta, depended upon the type of filler used.

Precipitation strengthening phases, *e.g.*, γ' or γ'', were not observed in the weld metal by SEM. Therefore, thin foils

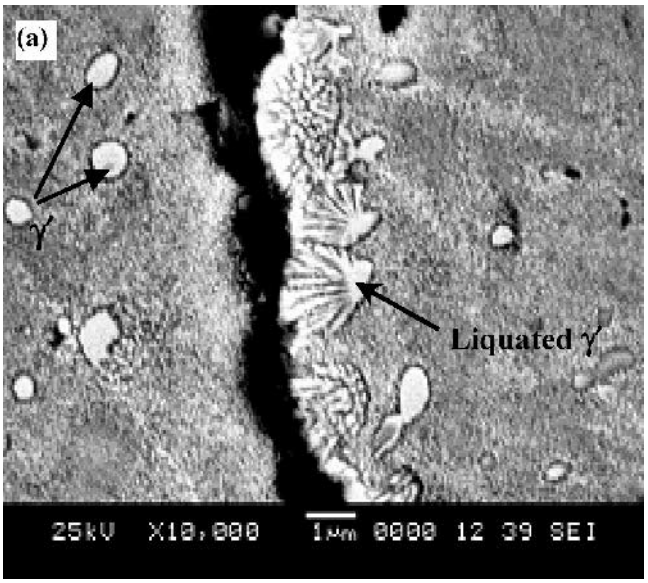

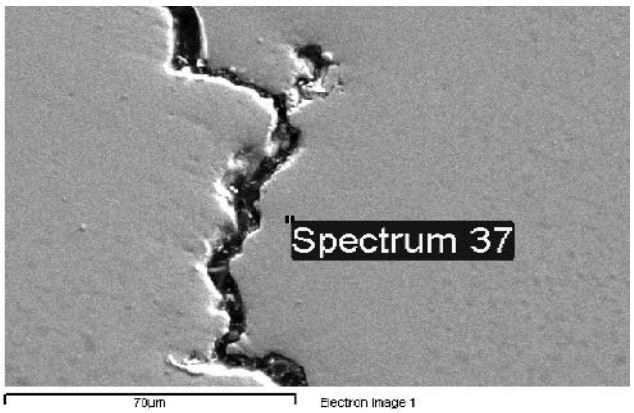

(*b*)

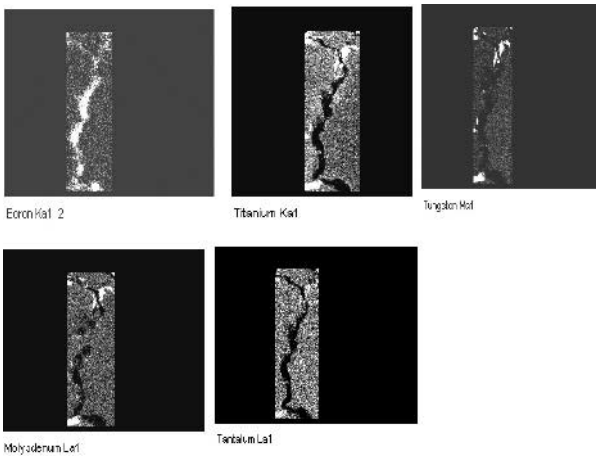

(*c*)

Fig. 7—Representative micrograph showing the (*a*) HAZ crack with liquated γ' on the cracked grain boundary of ST material welded with RENE-41 filler, (*b*) cracked grain boundary in the HAZ of ST material welded with C-263 filler, and (*c*) presence of boride on cracked grain boundary in X-ray map.

of the weld metal of welds made with the four filler alloys were examined by TEM. A representative TEM micrograph of fcc γ matrix of the C-263 weld metal and its selected-

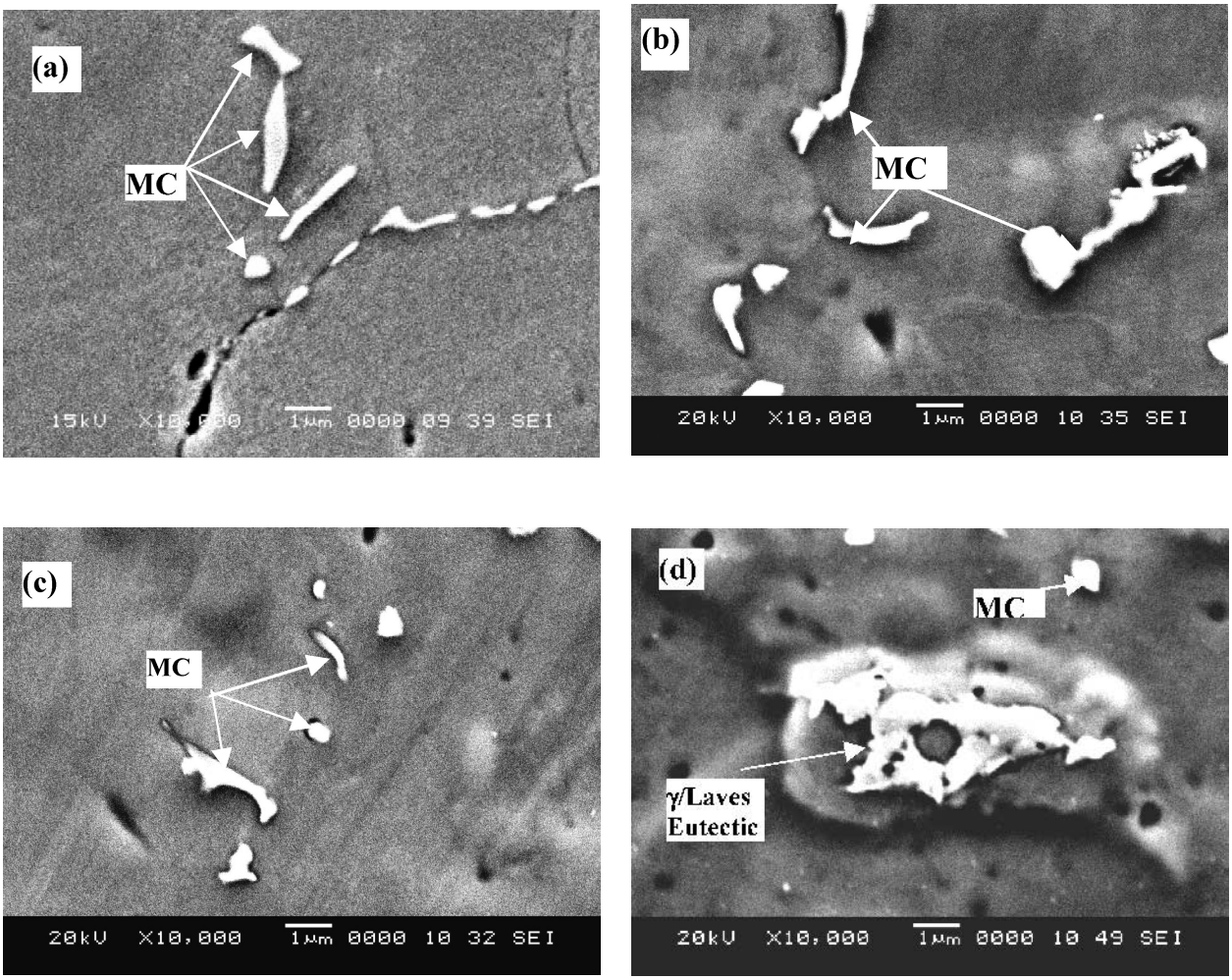

Fig. 8—Weld zone microstructure of (*a*) C-263 (ST), (*b*) RENE-41 (ST) material, (*c*) FM-92 (ST), and (*d*) IN-718 (ST).

Table II. EDS Analysis of γ/Laves Eutectic in IN-718 Weld

Elements (At. Pct)							
Al	Ti	Cr	Fe	Co	Ni	Nb	Mo
3.26	5.6	20.1	7.2	4.2	43.5	10.8	5.4

area diffraction pattern (SADP) with a [112] zone axis is shown in Figures 9(a) and (b), respectively. As shown in Figure 9(a), fine precipitates (~11 nm) were observed, which were identified to be γ' phase by their superlattice reflections shown in the SADP in Figure 9(b). The presence of γ' particles (~18 nm) along with grain boundary MC carbides was also observed in the TEM microstructure of the weld metal of RENE-41 filler welds. Fine precipitates (21 nm) were also observed in the weld metal of welds made with IN-718 filler, which were identified to be γ' by SADP analysis. However, the presence of the major precipitation strengthening phase in IN-718, bct-γ'', was not detected in the SADP. Only MC carbide precipitate particles were observed in the weld metal of welds made with FM-92 filler.

Precipitation in the weld metal resulted in the hardness of C263 and RENE 41 welds being significantly higher than those of FM 92 and IN-718 filler welds, as shown in Table III. To determine the origin of observed differences in the hardness, an attempt was made to determine the lattice mismatch between γ' and the γ matrix of the weld metal. For this, the weld metal was carefully separated from the weldment by a wire EDM machine and then examined by X-ray diffractometer. As the amount of weld metal was not sufficient, the usual method of electrochemically extracting the precipitates for the X-ray diffraction analysis could not be used and, hence, bulk weld-metal sample was used. Again, the evidence of superlattice reflection due to γ' was observed in C-263, RENE-41, and IN-718 welds. However, in FM-92 welds, no γ' precipitate reflections at all were observed by X-ray diffraction. Unfortunately, perhaps due to the small volume fraction of γ' precipitates, only low-angle γ' reflections could be identified with certainty and higher order reflections could not be identified unambiguously. Therefore, (110)-γ' superlattice reflection and (220)-γ matrix reflection were used to estimate the lattice parameters of γ' and γ matrix, and the lattice mismatch (δ) was estimated by[14]

$$\delta = (a_{\gamma'} - a_{\gamma})/a_{\gamma}$$

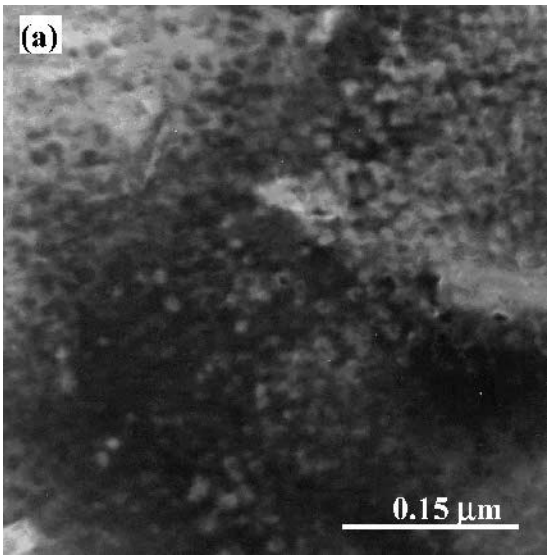

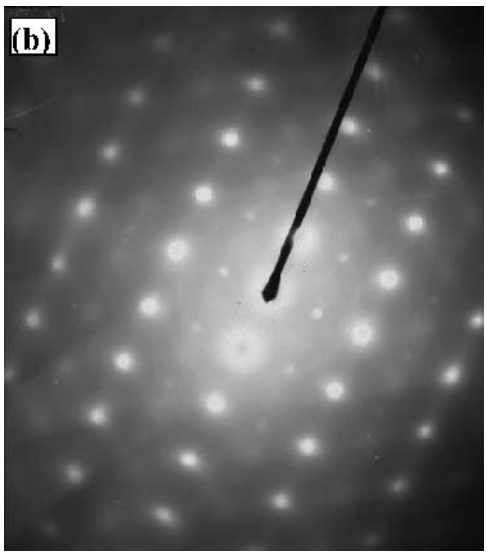

Fig. 9—(*a*) TEM micrograph of C263 (ST) weld zone showing γ' precipitates and (*b*) corresponding SADP of [112] zone showing fcc γ matrix and superlattice reflection of γ'.

Table III. Lattice Parameters and Lattice Mismatch in the Welds

Weld Metal (ST)	a_γ, Å (*hkl*—220)	$a_{\gamma'}$, Å (*hkl*—110)	$\delta = (a_{\gamma'} - a_\gamma)/a_\gamma$	Weld Hardness
C-263	3.5921	3.5429	−0.0137	373 ± 5
RENE-41	3.5988	3.5458	−0.0147	382 ± 3
IN-718	3.5960	3.5833	−0.0035	340 ± 5
FM-92	3.5827	no reflection	—	335 ± 6

where

a_γ' = constrained lattice parameter of γ' and

a_γ = constrained lattice parameter of γ.

The estimated lattice parameters and lattice mismatch along with the corresponding weld-metal hardness values are listed in Table III. It is seen that C263 and RENE-41 filler weld metal have a significantly larger negative lattice mismatch than that observed in IN-718 filler weld metal. It is also reflected in the larger hardness values of C263 and RENE-41 weld metal as compared to the IN-718 filler weld metal.

To determine if any element from the weld metal were diffusing into the HAZ, or if the weld metal was backfilling the HAZ cracks and was contributing to cracking, energy-dispersive X-ray analysis was carried out. However, no evidence of any element diffusing in the HAZ grain boundaries or backfilling the cracks from the weld metal was observed by X-ray chemical analysis, X-ray line scan, or X-ray mapping.

C. *Solidification Temperature Range and Solidus Temperature of Filler Alloys*

The different filler alloys will have different solidification temperature ranges and different solidus temperatures, which, combined with dilution from the parent metal during welding, will contribute to varying solidification temperature ranges during solidification. At the same weld cooling rate, a weld with a filler alloy whose solidification temperature range is wider would remain liquid for a longer period of time and, hence, is likely to be more susceptible to weld cracking. Also, a filler alloy with a higher solidus temperature than that of the base metal would solidify while the HAZ may still be liquid, and is likely to suffer cracking due to an increased level of welding stresses. Therefore, to determine if a difference in the solidification temperature range or solidus temperature has a role in influencing the cracking of welds made with different filler alloys, these parameters were evaluated. The solidus temperature (T_S), liquidus temperature (T_L), and consequently solidification temperature range of the base and weld metal was measured using a high-temperature differential scanning calorimeter. In these experiments, the heating trace best represents the liquidus temperature (T_L) of the weld because solidification in the fusion zone occurs by epitaxial growth on existing base metal grains and requires no undercooling. Thus, the use of heating trace avoids the undercooling associated with the cooling trace and the liquidus was readily apparent as an abrupt change in the trace. However, the microsegregation that might occur under the nonequilibrium solidification conditions during cooling of the fusion zone may lead to the build up of solute-rich liquid and the formation of secondary phases at lower temperatures that are best represented by the cooling portion of the DSC trace. Therefore, the solidification temperature range of the weld metal was measured by the liquidus temperature determined by the heating trace and the solidus temperature determined by the cooling trace. The solidification temperature range is represented as T_L-T_S, where T_S was taken as the intersection of the tangent to the cooling curve with the tangent to the base line. It is seen from the data in Table IV that the solidification temperature range of the weld metal is not affected by the type of filler used, being within a range of 8 °C for all four fillers and the IN 738 alloy. The Av. TCL values, however, ranged from 0.28 to over 13 mm.

Pronounced peaks corresponding to the solvus temperature of the major precipitating phase γ' were observed in the cooling curves of weld metals of welds made with C-263 and RENE-41. This would imply precipitation of γ', whereas

Table IV. High-Temperature DSC Data of the Base Material and Different Welds

Material (ST)	Solidus, T_s (°C)	Liquidus, T_L (°C)	Solidification Temperature Range, ΔT (°C)	Av. TCL (mm)
Base metal	1234	1340	106	—
C-263 weld	1257	1369	112	0.99
RENE-41 weld	1238	1348	110	0.92
FM-92 weld	1259	1368	109	0.281
IN-718 weld	1239	1343.3	104	0.28

a relatively shallow peak was noticed in the weld metals of FM-92 and IN-718 welds, which is indicative of a smaller volume fraction of γ' precipitates. Since the cooling rates of all the welds were the same, this would suggest that the precipitation rate in C-263 and RENE-41 is much faster than those in IN-718 and FM-92. This was reflected in the microstructure and the observed hardness values.

D. *HAZ Cracking Mechanism*

In all, the welds cracks were confined to the HAZ and no solidification cracking in the weld metal was present. The mode of cracking was mainly intergranular and the cracks did not enter the fusion zone. That is, cracks originated in the heat-affected zone. These cracks were always associated with liquated phases that were present in the preweld heat-treated materials. Liquation of some of the phases in HAZ, such as γ' and MC carbides, occurred by constitutional liquation proposed by Pepe and Savage.[11] If the solute forms a eutectic with the base metal, such as Nb from NbC in Ni, then the excessive concentration of the solute atoms may lower the melting temperature in the localized regions in the matrix to a low enough level for localized liquation to occur. In other words, the solid-state particle dissolution precedes the constitutional liquation.[16] The phases observed to have constitutionally liquated and contributed to HAZ cracking were γ', $\gamma + \gamma'$ eutectic, and MC carbides; in addition, lower melting temperature phases such as Zr carbosulfide and boride rich in molybdenum and chromium were also found to have liquated, and would have contributed to the HAZ cracking. Owczarski *et al.*[12] reported that in UDIMET 700 and WASPALOY, several types of particles, *e.g.*, MC, $M_{23}C_6$-type carbides, and borides, rapidly decomposed during the weld thermal cycle. Because of the consistently observed association of liquated regions with MC-type carbides, they concluded that this type of particle was a prime contributor to the melting reaction. Zirconium has been reported[17] to be involved in the formation of low melting phases in Ni-based alloys. Both B and Zr have a tendency to segregate to the grain boundaries due to their lower solubility in γ and γ', and they are also rejected in the residual liquid during the solidification process. Therefore, the region last to solidify is enriched in B and Zr, and phases that form in it have a lower melting point.[18] The Zr forms sulfide or sulfocarbide while excess boron is usually tied up by Mo, Ti, Cr, and Ni to form complex borides or M_3B_2.[19] This boride phase would be the source of boron at the grain boundaries, seen in Figures 7(b) and (c), and would contribute to HAZ cracking in Ni-base superalloys.[20] Kelly[21] suggested that the presence of boron in cast IN-718 caused the metallic carbides to wet grain boundaries and, thus, explained the deleterious effect of boron on HAZ cracking susceptibility. Boride and Zr-rich carbosulfide were observed on the HAZ cracks in this investigation.

The presence of liquated phases in the HAZ of IN-738LC welds made with different filler alloys in this study suggests that it is one of the major factors responsible for HAZ cracking. However, it does not explain the significant variation in HAZ cracking observed in welds made with different filler alloys (Figure 6), as the same liquating phases were present in the base metal of all the welds regardless of the filler alloy used. Furthermore, an extensive energy-dispersive X-ray analysis, X-ray line scanning, and X-ray mapping did not reveal any noticeable diffusion of elements from the weld metal in to the HAZs. The small variation in solidification temperature range and the solidus temperatures observed in different weld metals did not correlate with the cracking susceptibility data either. The only significant differences in the characteristics of welds made with different filler alloys were (1) the difference in the lattice mismatch between the γ' precipitates and γ matrix of the weld metal (Table IV) and (2) the hardness of the weld metal. The possible influence of these factors on HAZ cracking is considered next.

Table III shows that significantly large shrinkage strains would be present in the weld metal of the welds made with C-263 and RENE-41 fillers as compared to those present in the weld metal of weld made with IN-718 (mismatch between γ' and γ matrix of the fillers C-263 and RENE-41 is -0.0137 and -0.0147 as compared to -0.0035 in IN-718). Since the volume fraction of liquated phases in all the welds should be the same because of the same preweld microstructure of the base alloy and the use of identical thermal cycle, a larger amount of tensile stresses in the HAZ of C-263 and RENE-41 filler welds would result in a greater degree of HAZ cracking, as was observed in this study.

The hardness of the weld metal also seems to have influenced the HAZ cracking, as shown in Figure 10(a), in which the Av. TCL value is plotted against the weld metal hardness of different welds. From the hardness data (Figure 10(a)), it is apparent that the softer weld metal produced by using IN-718 and FM-92 is better capable of accommodating stresses generated during the welding process than the welds made with the other two filler alloys, C263 and RENE-41, the hardness values of which are higher. In addition to the lattice mismatch, the hardness of the weld metal would also be influenced by the size and volume fraction of the strengthening precipitates, which are a function of the concentration of (Ti + Al) and the kinetics of precipitation of the strengthening phase in it. This is reflected in Figure 10(b), which is a plot between the concentration of (Ti + Al) in the filler alloy and the Av TCL values. A stronger weld metal would not deform plastically to relieve the welding stresses and they would be transferred to the HAZ and may cause it to crack, as was observed in the welds made with C-263 and RENE-41 filler alloys. This would also explain why the UMT preweld-treated material with its softer base metal consistently suffered a smaller amount of HAZ cracking than the solution-treated material, which was harder, regardless of the filler alloys used. This is consistent with the suggestion of Borland Younger[22] that a weld metal with lower plastic resistance than the base metal is beneficial since the amount of stress that is needed to be accommodated by the

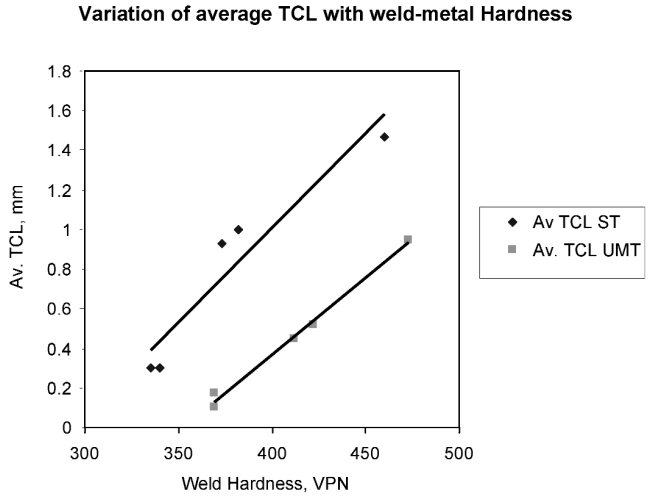

(*a*)

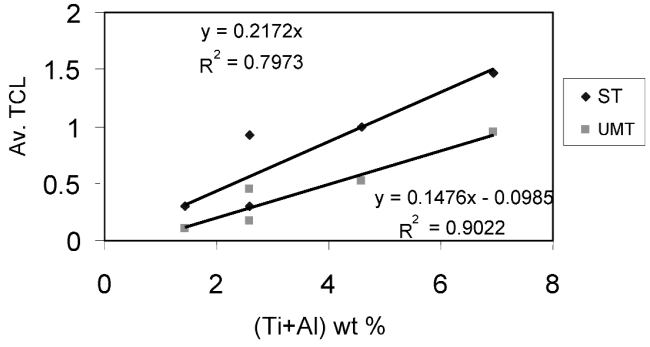

(*b*)

Fig. 10—(*a*) Variation of average TCL with hardness differential. (*b*) Av. TCL *vs* (Ti + Al) wt pct for ST and UMT heat treatments.

base metal is reduced, which in turn reduces the amount of cracking.

The main strengthening precipitate in C-263 and RENE 41 is γ', which has a very high precipitation rate, as indicated by the weld hardness values (Figure 10(a)). In IN-718 the volume fraction of γ' precipitates is only about 3 to 4 pct as compared to 13 to 15 pct of the main strengthening phase γ'', which has a relatively slow precipitation rate. The slower aging response of IN-718[23] and FM 92,[24] as compared to RENE 41, is illustrated in Figure 11. Unfortunately, the age-hardening information of C-263 alloy is not available in the literature. However, an indication of rapid precipitation of γ' phase in C-263 and RENE-41 was provided by the well-developed peaks corresponding to the solvus of γ' observed in thermograms obtained by DSC analysis. Since the weld thermal cycle was the same for all the welds, filler alloys with a slow precipitation hardening response, such as IN-718, would produce welds with softer weld metal as compared to those made with C263 and RENE-41, which have a very rapid precipitation hardening response.

Therefore, the present work suggests that the HAZ cracking of welds in IN-738 LC is associated with the liquation of the phases that are generally present in the microstructure of the base material. The extent of cracking, however, is controlled by the lattice mismatch between γ' and γ as

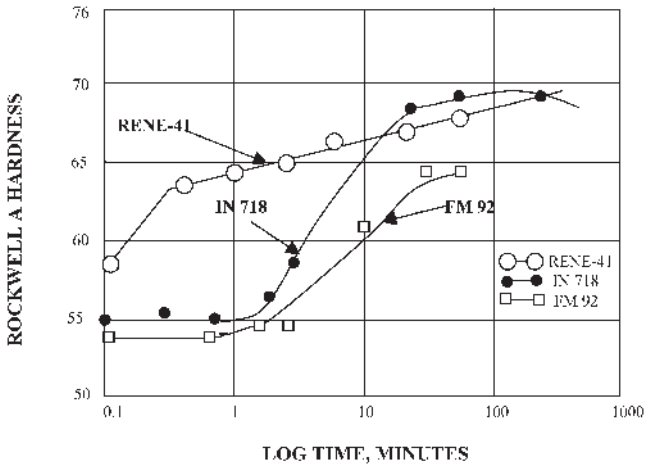

Fig. 11—Age-hardening response curves for three alloys. Note fast precipitation response of RENE'41 as compared to that of IN-718 and FM 92.[25]

well as the volume fraction of γ' (as a function of Ti + Al percentages and precipitation kinetics) in the weld metal, both of which depend upon the filler alloy and its aging response. This study also suggests that HAZ cracking in IN-738 can be significantly minimized by using suitable filler alloys, which have a relatively slower aging response and have a smaller negative lattice mismatch.

IV. SUMMARY AND CONCLUSIONS

The effect of using filler alloys with different Ti and Al concentrations on HAZ cracking in GTA-welded IN-738LC superalloy, in two preweld heat-treated conditions, was studied. The following observations were made.

1. All welds suffered cracking, which was intergranular in nature but was confined to the HAZ only, and the weld metal did not crack.
2. All cracks were associated with liquated phases, which were present in the base alloys in both heat-treated conditions.
3. The HAZ cracking increased with an increase in the lattice mismatch between the γ' precipitates and the γ matrix of the weld metal, as well as in the hardness of the weld metal. Welds made with filler alloys C-263 and RENE 41, both of which have a larger γ-γ' lattice mismatch and harder weld metal, were significantly more susceptible to HAZ cracking than FM-92 and IN-718 welds, which have a smaller γ-γ' lattice mismatch and a softer weld metal.
4. The HAZ in the autogenous weld had the highest degree of cracking and its hardness was also the highest.
5. A specially designed preweld heat treatment, which produced a softer base material, consistently suffered less HAZ cracking than that observed in the material that was given a conventionally used solution treatment, which produced a harder base material.
6. It is concluded that the use of filler alloys with a (a) slower aging response, (b) smaller lattice mismatch between the precipitating phase and the matrix, (c) smaller concentration of (Ti + Al) and (d) softer weld metal

would reduce the HAZ cracking susceptibility of IN-738LC welds.

ACKNOWLEDGMENTS

The authors thank the consortium of Manitoba aerospace industries and NSERC for the financial support. Thanks are also due to Standard Aero Co. (Winnipeg) for carrying out welding of the samples and to Dr. Henry Saari, Carleton University (Ottawa), for assistance with the DSC tests. The technical assistance of Mr. Dan McCooeye is thankfully acknowledged.

REFERENCES

1. W. Lin, J.C. Lippold, and W.A. Baeslack III: *Welding Res. Suppl*., 1993, Apr., pp. 135s-153s.
2. D.S. Duvall and W.A. Owczarski: *Welding J*., 1967, Sept., pp. 423s-432s.
3. R. Thamburaj, W. Wallace, and J.A. Goldak: *Int. Mater. Rev*., 1983, vol. 28, (1), pp. 1-22.
4. O.A. Ojo, N.L. Richards, and M.C. Chaturvedi: *Scripta Mater*., 2004, vol. 50, pp. 641-46.
5. A.K. Koul and R. Thamburaj: *Metall. Trans. A*, 1985, vol. 16A, pp. 17-26.
6. A. Thakur, N.L. Richards, and M.C. Chaturvedi: *Int. J. Joining Mater*., 2003, vol. 15 (4), pp. 21-25.
7. B. Jahnke: *Welding Res. Suppl*., 1982, Nov., pp. 343s-347s.
8. H. van Esch and W. Greaves: *ASM Int*., 1998, Oct., pp. 130-37.
9. P. Lowden, C. Pilcher, and J. Liburdi: *Proc. Int. Conf. on Gas Turbines and Aeroengine Congr. and Expo*., Orlando, FL, June 3–6, 1991, The American Society of Mechanical Engineers, New York, NY, 1991, pp. 303-13.
10. C.Y. Su, C.P. Chou, B.C. Wu, and W.C. Lih: *J. Mater. Eng. Performance*, 1997 vol. 6 (5), pp. 619-27.
11. W.F. Savage and J.J. Pep: *Welding J., Res. Suppl*., 1967, vol. 46 (9), pp. 411s-422s.
12. W.A. Owczarski, D.S. Duvall, and C.P. Sullivan: *Welding Res. Suppl*., 1966, Apr., pp. 145s-155s.
13. B. Radhakrishnan and R.G. Thompson: *Metall. Trans. A*, 1991, vol. 22A, pp. 887-902.
14. D.F. Lahrman, R.D. Field, R. Darolin, and H.L. Fraser: *Acta Metall*., 1988, vol. 36 (5), pp. 1309-20.
15. B.H. Yoon, Y.S. Ahn, and C.H. Lee: *Iron Steel Inst. Jpn. Int*., 2002, vol. 42 (2), pp. 178-83.
16. J.C. Lippold, W.A. Baeslack III, and I. Varol: *Welding Res. Suppl*., 1992, Jan., pp. 1s-7s.
17. R.E. Pease: *Welding J., Res. Suppl*., 1957, vol 36, pp. 330s-334s.
18. K. Saito, M. Aoki, H. Kondo, and N. Ikeda: *Iron Steel Inst. Jpn. Int*., 1987, pp. 664-72.
19. D.S. Duvall and W.A. Owczarski: *Welding Res*., 1967, vol. 32, pp. 423s-432s.
20. W.A. Owczarski: *Welding Res. Council*, 1969, pp. 6-23.
21. T.J. Kelly: *Welding J*., 1989, vol. 68, pp. 44s-51s.
22. J.C. Borland and R.N. Younger: *Br. Welding J., Res. Suppl*., 1960, Jan., pp. 22-59.
23. H.L. Eiselstein: *Am. Soc. Testing Mater., Tech. Pub*., 1965, No. 369, pp. 62-79.
24. M.C. Chaturvedi: University of Manitoba, Winnipeg, unpublished research, 2004.